Macromolecular Rapid Communications
www.mrc-journal.de

Benzoxazine/Triphenylamine-Based Dendrimers Prepared through Facile One-Pot Mannich Condensations

*Ruey-Chorng Lin, Mohamed Gamal Mohamed, and Shiao-Wei Kuo**

A series of thermally polymerizable dendrimers of various generations, equipped with triphenylamine (TPA) and benzoxazine (BZ) groups, is synthesized through facile one-pot Mannich condensations of N^1,N^1-bis(4-aminophenyl)benzene-1,4-diamine (TPA–3NH_2, as the core group), 4-(bis(4-aminophenyl)amino)phenol (TPA–2NH_2–OH, as the AB_2 branching group), and CH_2O in 1,4-dioxane. The ratios of the integrated areas in the ^1H nuclear magnetic resonance spectra of these dendrimers are consistent with the theoretical numbers of protons, suggesting their successful syntheses. Bathochromic shifts of signals are evident in the UV–vis and photoluminescence spectra upon increasing the generation of the TPA–BZ dendrimers, consistent with an increase in the effective conjugation length. The TPA–BZ dendrimers are able to undergo thermal polymerization and display unique optical physical properties, resulting in thermoset TPA networks after thermal ring-opening polymerization.

1. Introduction

Dendrimers have many attractive properties—uniform molecular weight, nanoscale dimensions, symmetrical chemical structures, modifiable terminal groups, and low viscosity relative to linear polymeric counterparts—that continue to gain them much attention.[1] Indeed, dendrimers have found applicability in many fields, including drug delivery, nonlinear optical devices, and sensor devices.[2] In addition, triphenylamine (TPA), with its unique two-photon absorption ability, has also been applied widely in, for example, electron transition devices, optoelectronic devices, and the hole injection/transport materials of organic light-emitting diodes.[3] Conjugated polymers containing TPA groups can display enhanced material performance (e.g., greater conjugated length, solvent-resistance, thermal stability, and mechanical strength) when these TPA groups are located in either the main chain or the side chains.[4]

Benzoxazine (BZ) monomers can undergo thermal ring-opening polymerization without forming byproducts and without needing any additional catalysts; the resulting polymers can display high flame retardancy, high chemical resistance, and low surface free energies.[5] Many academic studies have revealed the enhanced performance of polybenzoxazines after incorporating reactive functional groups into the BZ monomers,[6] blending various inorganic/organic compounds with the monomers,[7] and increasing the number of BZ functional groups or polymerizable functional groups in the monomer,[6f] all of which can increase the crosslinking density of the products. Benzoxazines are typically prepared through Mannich condensation: a primary amino group is activated through reaction with formaldehyde, resulting in an activated formaldehyde-amine derivative that reacts precisely with a phenol group to form the BZ.[8] Hence, we suspected that a dendrimer possessing such activated terminal groups might react directly with the phenol groups of additional branching units, thereby avoiding the need for complicated and tedious protection/deprotection strategies to increase the generation of the dendrimer. TPA–BZ dendrimers, featuring TPA and BZ moieties, possess unique optical physical properties and can undergo thermal ring-opening polymerization, resulting in the thermoset TPA networks.[9] In a previous study, we prepared a novel linear polybenzoxazine containing TPA moieties in the main chain; because of enhanced thermal stability and solvent-resistance, this high-performance polymer was a suitable hole injection/transport material in organic light-emitting diodes.[9b]

In this study, we examined the effects of incorporating TPA moieties into dendrimer structures, namely at the core and branching units. We employed BZ units, capable of ring-opening polymerization, as bridges between each TPA molecule and the terminal groups of the dendrimers. A series of TPA–BZ dendrimers of generation zero (DG0), one (DG1), two (DG2), and three (DG3) was synthesized through facile one-pot Mannich condensations of TPA–3NH_2 (**Scheme 1**A; as core groups), TPA–2NH_2–OH (Scheme 1B; as branching groups), CH_2O, and phenol in 1,4-dioxane. A protection/deprotection strategy was, however, necessary to prepare TPA–2NH_2–OH because it was difficult to synthesize directly.[10] To the best of our knowledge, the incorporation of BZ groups into dendrimer structures through such a convenient synthetic strategy has not been reported previously.

Dr. R.-C. Lin, Dr. M. G. Mohamed, Prof. S.-W. Kuo
Department of Materials and Optoelectronic Science
Center for Nanoscience and Nanotechnology
National Sun Yat-Sen University
Kaohsiung 804, Taiwan
E-mail: kuosw@faculty.nsysu.edu.tw

DOI: 10.1002/marc.201700251

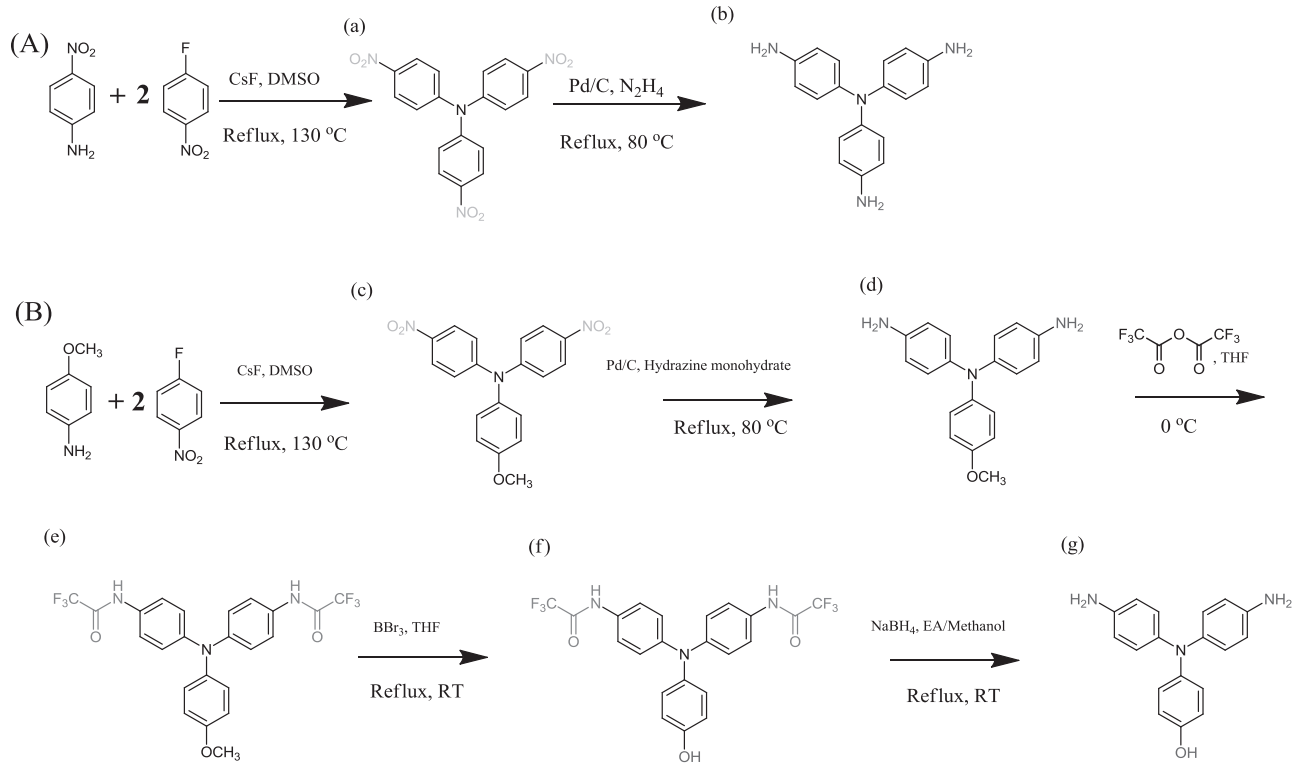

Scheme 1. Syntheses of A) a) TPA–$3NO_2$ and b) TPA–$3NH_2$, and B) c) TPA–$2NO_2$–OCH_3, d) TPA–$2NH_2$–OCH_3, e) TPA–$2NHCOCF_3$–OCH_3, f) TPA–$2NHCOCF_3$-OH, and g) TPA–$2NH_2$–OH.

2. Results and Discussion

2.1. Preparation of TPA–BZ Dendrimers of Various Generations

We designed the source of the TPA branching unit to be an AB_2 molecule possessing one OH group and two protected primary amino groups (TPA-2Protected-OH). The OH groups of three TPA-2Protected-OH units and formaldehyde would react with the three primary amino groups of TPA–$3NH_2$ through Mannich condensations; the protected functional groups of these TPA-2Protected-OH units (terminal groups of the dendrimer) would then be deprotected to reveal six reactive primary amino groups as terminal units for the generation-one dendrimer (DG1). Phenol and formaldehyde would then be added for Mannich reactions with the six terminal NH_2 groups of DG1, resulting in the DG1 derivative presenting BZ terminal groups. The two reactive primary amino groups of the TPA branching unit (TPA–$2NH_2$–OH) would be protected when its OH group reacted with the terminal reactive groups of the dendrimers; this approach would guarantee that only the OH groups of the TPA-2Protected-OH units reacted with the terminal reactive primary amino groups of the dendrimers. Zhang et al. reported that the kinetics of Mannich condensation of a primary amine, a phenol, and CH_2O (Scheme S1, Supporting Information) involve three steps: (i) degradation of poly(oxymethylene) glycol to the methylene glycol, (ii) dehydration of the methylene glycol into CH_2O, and (iii) reaction of CH_2O and the Mannich base to form the BZ. Step (ii) is the rate-controlling step.[8] According to this mechanism for Mannich condensation, the characteristics of step (i) can be exploited such that the primary amino groups of the dendrimers (the core groups or the terminal groups) react specifically with formaldehyde to form formaldehyde-amine derivatives initially. As a result, the two primary amino groups of TPA–$2NH_2$–OH units would not need to be protected, because the OH group of the TPA–$2NH_2$–OH unit will react with a formaldehyde-amine derivative of the terminal group of the dendrimer, resulting in Mannich base molecules or BZ rings forming to connect the TPA branching units and dendrimers. Finally, the Mannich base moieties formed between the TPA branching units and dendrimers would become BZ rings through reactions with the free formaldehyde in step (iii) of the Mannich condensation (**Scheme 2**). In other words, the OH groups of TPA–$2NH_2$–OH units would react with the formaldehyde-amine derivatives of the dendrimers to form the BZ ring bridge unit of each TPA group in the dendrimer structure. As a result, TPA–$2NH_2$–OH can be used directly, instead of TPA-2Protected-OH, for the dendrimer synthesis. Accordingly, we suspected that we could synthesize dendrimers containing TPA and BZ moieties (TPA–BZ dendrimers) through the facile one-pot synthesis displayed in Scheme S2 (Supporting Information), obviating the need for a complicated protection/deprotection approach.

In this study, we prepared TPA–BZ dendrimers of four different generations through facile one-pot Mannich condensations of TPA–$3NH_2$ (as a core group, Scheme 1A; Figures S1–S4, Supporting Information), TPA–$2NH_2$–OH (as branching groups, Scheme 1B; Figures S5–S9, Supporting Information), CH_2O, and phenol in 1,4-dioxane (Scheme 2). Fourier transform

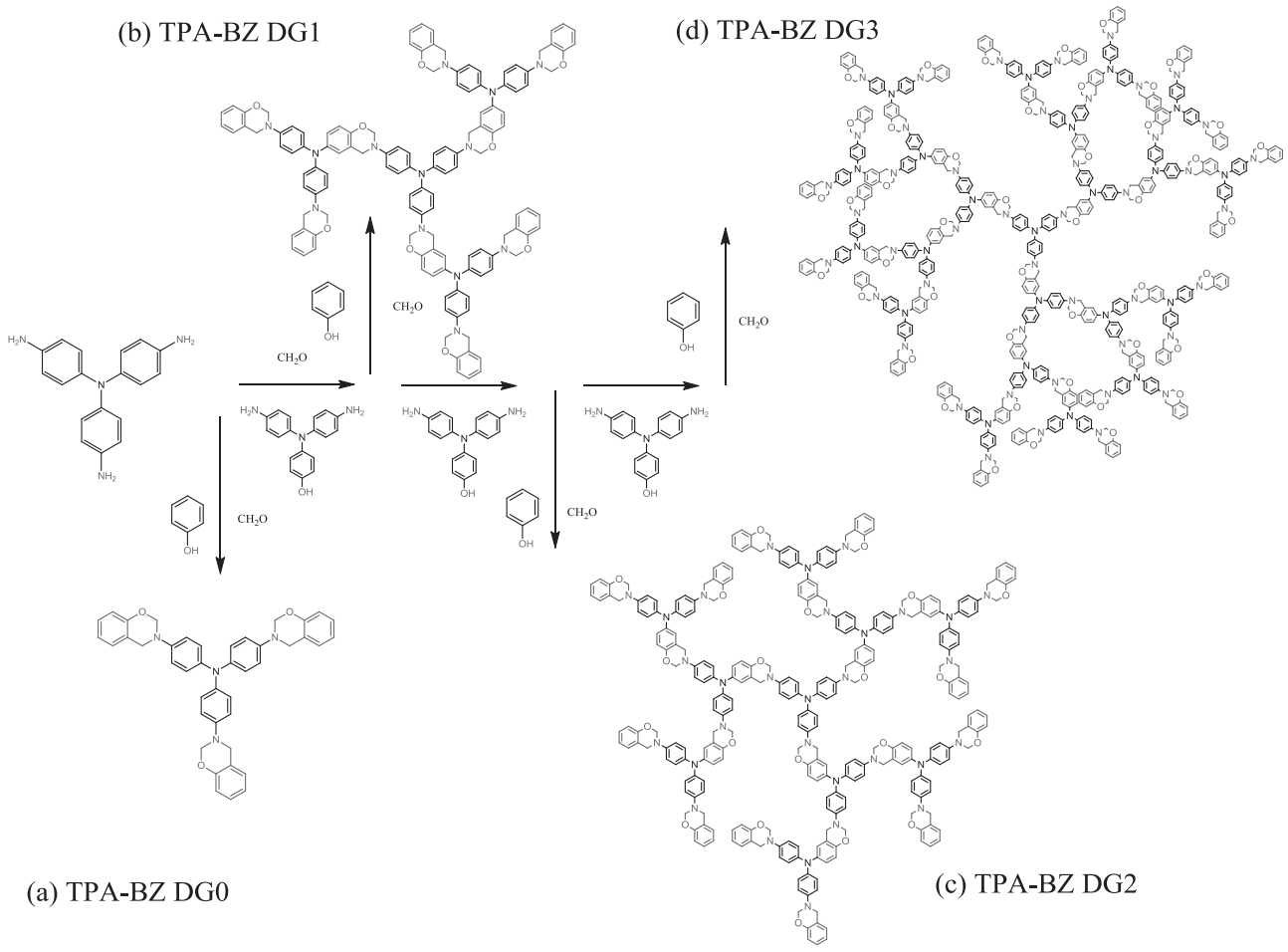

Scheme 2. Synthesis of TPA–BZ dendrimers of various generations: a) TPA–BZ DG0, b) TPA–BZ DG1, c) TPA–BZ DG2, d) TPA–BZ DG3, and e) possible higher-generation TPA–BZ.

infrared (FTIR), ^{1}H and ^{13}C nuclear magnetic resonances (NMR), and mass-analyzed laser desorption ionization/time-of-flight (MALDI-TOF) mass spectra confirmed the chemical structures of these TPA–BZ dendrimers. **Figure 1** presents the ^{1}H NMR spectra of all of the TPA–BZ dendrimers in DMSO-d_6. Two clear sharp signals appeared at 4.59 and 5.38 ppm for the CC**H**$_2$N and OC**H**$_2$N groups, respectively, of the BZ units of the TPA–BZ dendrimers. The integrated areas of these two peaks were 2.00 and 2.02, respectively (Figure S10, Supporting Information); their ratio is close to one, indicating the high purity of TPA–BZ DG2. The theoretical number of protons in TPA–BZ DG2 providing these two peaks is 84 (21 BZ rings). The integrated area was 8.41 for the designated protons of the aromatic rings (159 protons). The integrated area of a ^{1}H NMR spectral signal is actual measurement data, while the number of protons for the compound is theoretical data; the ratios of integrated areas and numbers of protons must remain constant for a given compound. This approach is often used with ^{1}H NMR spectroscopy to confirm chemical structures. Here, we integrated the two peaks **a** and **b** of the BZ ring and the designated protons of the aromatic rings to confirm the chemical structure of TPA–BZ DG2. **Table 1** presents the theoretical numbers of protons and the corresponding integrated areas of these signals in the ^{1}H NMR spectra of the TPA–BZ dendrimers. For TPA–BZ DG2, the ratios of the integrated areas and the theoretical number of protons for the BZ rings B (including CC**H**$_2$N and OC**H**$_2$N groups) and aromatic rings T (designated protons in chemical structure) were 0.0479 and 0.0476, respectively; the value of B/T of 1.01 indicates that TPA–BZ DG2 was synthesized successfully to contain 21 BZ rings. Table 1 reveals that the values of B/T for TPA–BZ DG1 and TPA–BZ DG3 were 1.03 and 1.02, respectively, confirming that they had also been synthesized successfully and that the numbers of BZ rings and terminal groups for these two compounds were consistent with their theoretical constructions. Figure 1B presents the ^{13}C NMR spectra of all of the TPA–BZ dendrimers in DMSO-d_6. The peaks at 49.39 and 79.21 ppm represent the C**C**H$_2$N and O**C**H$_2$N groups of the TPA–BZ dendrimers. Each of these spectra features the two characteristic peaks of the BZ rings, confirming that the BZ rings were incorporated successfully into the TPA–BZ dendrimers as connection and terminal groups.

Figure S11 (Supporting Information) presents the FTIR spectra of all of the TPA–BZ dendrimers recorded at room temperature. The characteristic adsorption peaks of the BZ moieties appeared at 1225 (asymmetric COC stretching), 1338 (CH2

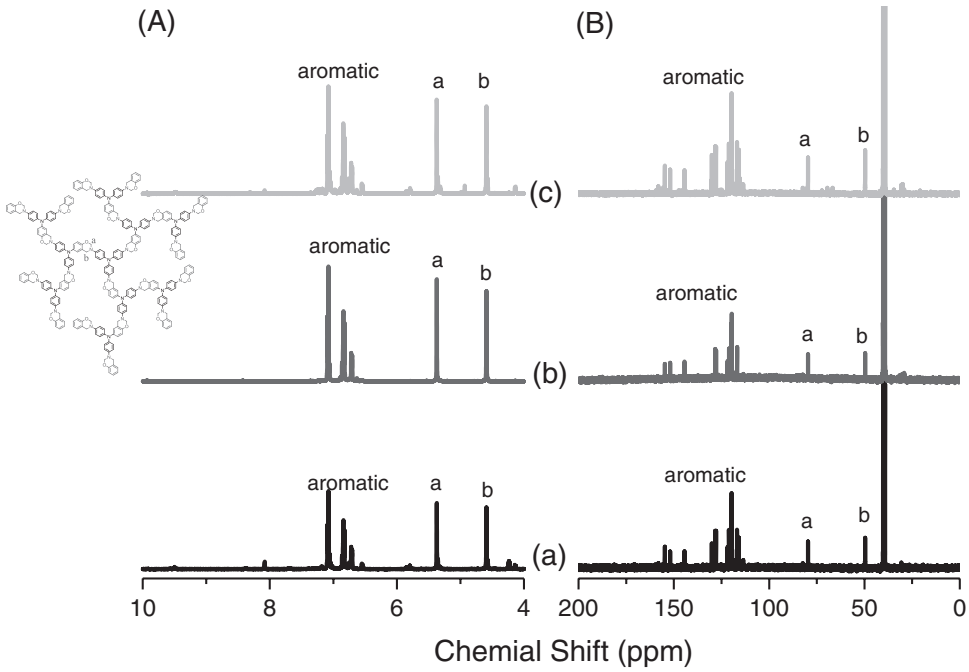

Figure 1. A) ^{1}H and B) ^{13}C NMR spectra of a) TPA–BZ DG1, b) TPA–BZ DG2, and c) TPA–BZ DG3.

wagging), and 941 and 1499 (vibrations of trisubstituted benzene ring) cm^{-1}, consistent with the successful incorporation of the BZ groups in each of the TPA–BZ dendrimers. We recorded MALDI-TOF mass spectra to determine the molecular weights of the TPA–BZ dendrimers. Figure S12 (Supporting Information) displays the MALDI-TOF mass spectrum of TPA–BZ DG0; the signal for the $[M + H]^+$ ion at m/z 644.81 is in good agreement with the theoretical calculation (m/z 644.76), suggesting that TPA–BZ DG0 had been synthesized successfully. Notably, several peaks appeared below the signal for the molecular ion, with a reducing rate of multiples of 12, similar to the rule of $[M + H - 12n]^+$ observed previously for the decomposition of BZ monomers during MALDI-TOF mass spectral measurements.[11] Figure S13 (Supporting Information) presents the MALDI-TOF mass spectrum of TPA–BZ DG1; again, many signals appeared below that of the molecular ion; presumably, TPA–BZ DG1 decomposed during the measurement, following a similar rule of $[M + H - 12n]^+$. As the number of generations of the TPA–BZ dendrimers increased, the number of BZ units in the compounds increased, making the TPA–BZ dendrimers less stable during mass spectral measurement. Therefore, not surprisingly, we did not observe molecular ions in the MALDI-TOF mass spectra of TPA–BZ DG2 and TPA–BZ DG3.

2.2. UV–Vis Absorption and PL Emission Spectra of TPA–BZ Dendrimers

We used UV–vis absorption and PL emission spectroscopy to investigate the photophysical properties of our TPA–BZ dendrimers. **Figure 2**A presents the UV–vis absorption spectra for TPA, TPA–BZ DG1, TPA–BZ DG2, and TPA–BZ DG3, each at a concentration of 10^{-4} M in THF. Figure 2A-a reveals a characteristic absorption peak centered at 299 nm for pristine TPA; we ascribe it to the locally excited (LE) π–π^* transition. Figure 2A-b reveals three characteristic absorption peaks at 255, 281, and 301 nm for TPA–BZ DG1. We attribute the signal at 255 nm to the high-energy π–π^* transition, and the other two at 281 and 301 nm to the LE π–π^* transition and intramolecular charge transfer (ICT) π–π^* transition, respectively, arising from electron transfer from the relatively strongly electron-donating TPA moieties to the relatively weakly electron-donating BZ moieties, as a hybridized local and charge-transfer (HLCT) transition.[12] A small bathochromic shift of the signals in the absorption spectrum occurred upon increasing the generation of the TPA–BZ dendrimer, presumably because of the increase in the conjugation length. Notably, the wavelengths and intensities of the signals near 281 nm in the absorption spectra both increased upon

Table 1. The calculated results of integrated areas based on ^{1}H NMR spectrum for TPA–BZ dendrimers.

Sample	BZ ring				Aromatic ring			Ratio
	BZ rings	Protons	Area	Area/protons (*B*)	Protons	Area	Area/protons (*T*)	(*B*)/(*T*)
TPA–BZ DG1	9	36	4.09	0.1136	69	8.11	0.1106	1.03
TPA–BZ DG2	21	84	4.02	0.0479	159	8.41	0.0476	1.01
TPA–BZ DG3	45	180	4.10	0.0228	339	8.92	0.0223	1.02

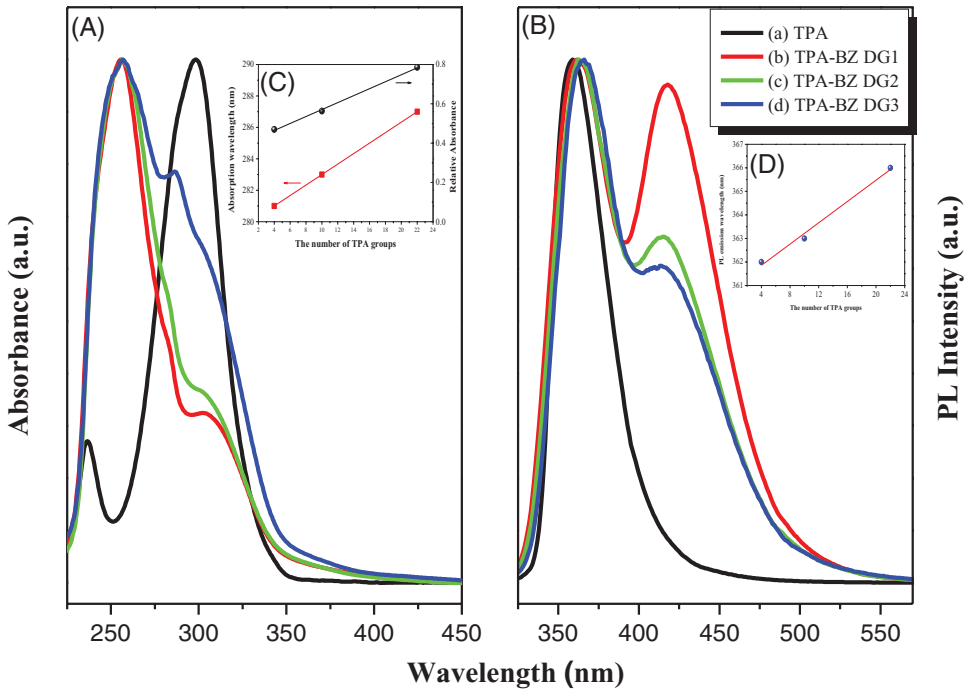

Figure 2. A) UV–vis absorbance and B) PL (excitation wavelength: 300 nm) spectra of a) TPA, b) TPA–BZ DG1, c) TPA–BZ DG2, and d) TPA–BZ DG3, as solutions in THF at a concentration of 10^{-4} M. C) Absorption wavelength and relative absorbance in UV–vis spectra. D) PL emission wavelength plotted with respect to the number of TPA groups.

increasing the number of TPA units in the TPA–BZ dendrimers (Figure 2C). Figure 2B presents the PL emission spectra for TPA, TPA–BZ DG1, TPA–BZ DG2, and TPA–BZ DG3, each at a concentration of 10^{-4} M in THF, with excitation at 300 nm. Figure 2B-a reveals an emission peak centered at 359 nm for pristine TPA, resulting from the LE π–π^* transition. Figure 2B-b reveals two PL emission peaks for TPA–BZ DG1 at 362 and 418 nm (peaks L and H, respectively) that possibly resulted from an HLCT transition and an aggregation occurred respectively. Upon increasing the generation of the TPA–BZ dendrimers, peak L in the PL emission spectrum shifted from 362 to 366 nm; this small bathochromic shift possibly resulted from a greater conjugation length.[13] Prasad et al. reported that as the number of branched TPA derivatives increases, bathochromic shifts can be observed in UV–vis absorption and one-photon emission spectra, and the TPA cross-section can be enhanced[14]; these phenomena are due to enhanced vibronic coupling, as has been determined theoretically.[15] Notably, the wavelength of peak L in the PL emission spectrum increased upon increasing the number of TPA units in the TPA-BZ dendrimers (Figure 2D). Therefore, the phenomenon of bathochromic shifts in the UV–vis absorption and PL emission spectra upon increasing the generation of the TPA-BZ dendrimers was possibly due to the increase in the effective conjugation length.[14,16] Interestingly, peak H in the PL emission spectrum underwent a small hypochromic shift from 418 to 414 nm with a decreasing PL emission intensity upon increasing the number of generations of the TPA–BZ dendrimers; this effect was possibly the result of aggregation of the dendrimers. The intensity of peak H of TPA–BZ DG1 was higher than that of TPA–BZ DG3, presumably because TPA–BZ DG1 is relatively small molecule and, therefore, aggregation can occur more readily. In contrast, TPA–BZ DG3 is bulky and more difficult to aggregate, relative to the lower-generation dendrimers TPA–BZ DG1 and TPA–BZ DG2.[17]

2.3. Thermal Behavior of TPA–BZ Dendrimers

We used differential scanning calorimetry (DSC) to investigate the thermal behavior of our TPA–BZ dendrimers. **Figure 3**A presents DSC traces of the uncured TPA–BZ dendrimers of various generations. The trace of each of the three TPA–BZ dendrimers features a sharp and symmetrical exothermic peak, with the center temperature in the range from 231 to 235 °C, considerably lower than those of the conventional Pa-type BZ monomer (263 °C)[18] and TPA derivatives featuring mono- or difunctional BZ moieties (248–270 °C).[8,19] Thus, our dendrimers were all of high purity and had the ability to undergo thermal ring-opening polymerization at temperatures much lower than those of typical BZ monomers. Scheme S3 (Supporting Information) presents a possible chemical structure of the TPA–BZ dendrimer after thermal curing. The DSC traces also reveal that the reaction heat increased upon increasing the generation of the TPA–BZ dendrimer. Thus, increasing the number of BZ rings in the TPA–BZ dendrimers enhanced both the degree of thermal curing and the reaction heat.

We combined FTIR spectroscopy, DSC, and TGA to investigate the thermal ring-opening polymerization behavior of our TPA–BZ dendrimers. We used DSC to monitor the thermal polymerization behavior for TPA–BZ DG2 before and after thermal curing (Figure 3B). Figure 3B-a presents the DSC thermogram of uncured TPA–BZ DG2; the sharp exothermic

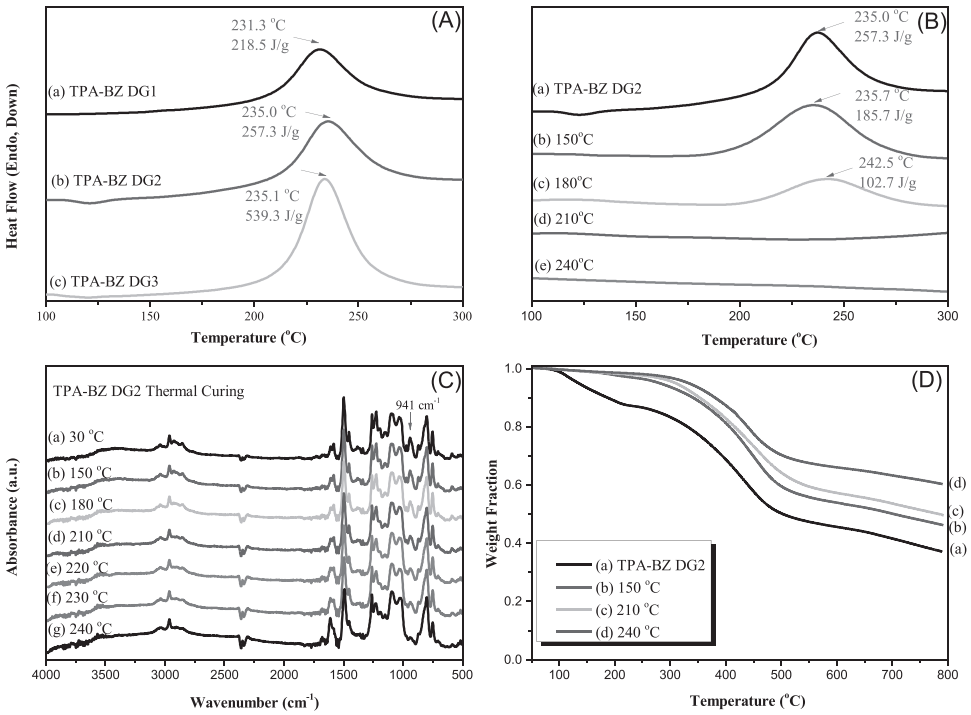

Figure 3. A) DSC traces of uncured TPA–BZ dendrimers: a) TPA–BZ DG1, b) TPA–BZ DG2, and c) TPA–BZ DG3. B) DSC traces of uncured TPA–BZ DG2. C) FTIR spectra of TPA–BZ DG2. D) TGA analyses of TPA–BZ DG2 recorded after each curing stage.

peak was centered at 235.0 °C and the enthalpy heat of reaction was 257.3 J g^{-1}. The enthalpy heat of reaction for the exothermic peak decreased gradually upon increasing the curing temperature, finally disappearing at 240 °C, implying that the full curing state of the polybenzoxazine had been reached. We recorded FTIR spectra to examine the thermal polymerization behavior of TPA–BZ DG2 before and after curing (Figure 3C). Prior to curing, the characteristic adsorption peaks of the BZ moieties of TPA–BZ DG2 appeared at appeared at 1225 and 941 cm^{-1}. The latter disappeared completely from the TPA–BZ DG2 spectrum after thermal curing at 240 °C (Figure 3C-g), consistent with the DSC analysis. We also employed TGA to monitor the thermal polymerization behavior of the TPA–BZ dendrimers. Figure 3D presents the TGA traces of TPA–BZ DG2 before and after thermal curing at various temperatures. The values of T_{d5} and char yield both increased upon increasing the thermal curing temperature, due to the greater crosslinking density. The complete thermal curing of TPA–BZ DG2 at 240 °C led to a value of T_d of 332.4 °C, and a char yield (60.6 wt%) significantly higher than that (43.0 wt%) for the model Pa-type of BZ. The thermal curing behavior of TPA–BZ DG1 and TPA–BZ DG3 was similar; for brevity, the results are not shown here.

3. Conclusions

TPA–BZ dendrimers have been synthesized using facile one-pot Mannich condensations. NMR and FTIR spectroscopic analyses revealed that the TPA–BZ dendrimers had structures consistent with their expected designs. DSC and TGA analyses revealed that the TPA–BZ dendrimers had low polymerization temperatures and formed crosslinked networks of high thermal stability, relative to those of the conventional Pa-type BZ monomer. We observed bathochromic shifts in the UV–vis and PL spectra upon increasing the generation of the TPA–BZ dendrimer, presumably because the effective conjugation length increased accordingly.

Supporting Information

Supporting Information is available from the Wiley Online Library or from the author.

Acknowledgements

This work was financially supported by the Ministry of Science and Technology, Taiwan, under contracts MOST103-2221-E-110-079-MY3 and MOST105-2221-E-110-092-MY3.

Conflict of Interest

The authors declare no conflict of interest.

Keywords

benzoxazine, dendrimer, thermal curing, triphenylamine

Received: April 18, 2017
Revised: May 22, 2017
Published online:

[1] a) G. R. Newkome, Z. Q. Yao, G. R. Baker, V. K. Gupta, *J. Org. Chem.* **1985**, *50*, 2003; b) D. A. Tomalia, H. Baker, J. Dewald, M. Hall, G. Kallos, S. Martin, J. Roeck, J. Ryder, P. Smith, *Polym. J.* **1985**, *17*, 117; c) D. A. Tomalia, A. M. Naylor, W. A. Goddard, *Angew. Chem., Int. Ed.* **1990**, *29*, 138; d) J. M. J. Fréchet, *Science* **1994**, *263*, 1710; e) S. K. Yang, S. C. Zimmerman, *Macromolecules* **2015**, *48*, 2504.

[2] a) P. Kesharwani, K. Jain, N. K. Jain, *Prog. Polym. Sci.* **2014**, *39*, 268; b) M. J. Cho, D. H. Choi, P. A. Sullivan, A. J. P. Akelaitis, L. R. Dalton, *Prog. Polym. Sci.* **2008**, *33*, 1013; c) D. Astruc, E. Boisselier, C. Ornelas, *Chem. Rev.* **2010**, *110*, 1857.

[3] a) H. M. Kim, B. R. Cho, *Chem. Commun.* **2009**, 153; b) Y. Shirota, *J. Mater. Chem.* **2000**, *10*, 1; c) Z. J. Ning, H. Tian, *Chem. Commun.* **2009**, 5483.

[4] a) M. Pawlicki, H. A. Collins, R. G. Denning, H. L. Anderson, *Angew. Chem., Int. Ed.* **2009**, *48*, 3244; b) X. Yang, S. W. Yao, M. Yu, J. X. Jiang, *Macromol. Rapid Commun.* **2014**, *35*, 834.

[5] a) W. F. Zhang, P. Froimowicz, C. R. Arza, S. Ohashi, Z. Xin, H. Ishida, *Macromolecules* **2016**, *49*, 7129; b) N. N. Ghosh, B. Kiskan, Y. Yagci, *Prog. Polym. Sci.* **2007**, *32*, 1344; c) S. Ohashi, J. Kilbane, T. Heyl, H. Ishida, *Macromolecules* **2015**, *48*, 8412; d) M. G. Mohamed, R. C. Lin, K. C. Hsu, W. Zhang, X. Zhong, S. W. Kuo, in *Advanced and Emerging Polybenzoxazine Science and Technology* (Eds: H. Ishida, P. Froimowicz), Elsevier, Amsterdam **2017**, Ch. 12, p. 205.

[6] a) J. Liu, H. Ishida, *Macromolecules* **2014**, *47*, 5682; b) K. Zhang, J. Liu, H. Ishida, *Macromolecules* **2014**, *47*, 8674; c) Y. Chen, L. K. Lin, S. J. Chiang, Y. L. Liu, *Macromol. Rapid Commun.*, **2016**, DOI: 10.1002/marc.201600616; d) R. Kudoh, A. Sudo, T. Endo, *Macromolecules* **2010**, *43*, 1185; e) Y. S. Ye, Y. J. Huang, F. C. Chang, Z. G. Xue, X. L. Xie, *Polym. Chem.* **2014**, *5*, 2863; f) R. C. Lin, M. G. Mohamed, K. C. Hsu, J. Y. Wu, Y. R. Jheng, S. W. Kuo, *RSC Adv.* **2016**, *6*, 10683; g) W. H. Hu, K. W. Huang, S. W. Kuo, *Polym. Chem.* **2012**, *3*, 1546.

[7] a) C. C. Yang, Y. C. Lin, P. I. Wang, D. J. Liaw, S. W. Kuo, *Polymer* **2014**, *55*, 2044; b) M. G. Mohamed, R. C. Lin, S. W. Kuo, in *Advanced and Emerging Polybenzoxazine Science and Technology* (Eds: H. Ishida, P. Froimowicz), Elsevier, Amsterdam **2017**, Ch. 36, p. 725; c) M. G. Mohamed, S. W. Kuo, *Polymers* **2016**, *8*, 225; d) H. K. Fu, C. F. Huang, S. W. Kuo, H. C. Lin, D. R. Yei, F. C. Chang, *Macromol. Rapid Commun.* **2008**, *29*, 1216; e) F. B. Meng, H. Ishida, X. B. Liu, *RSC Adv.* **2014**, *4*, 9471.

[8] a) Y. Y. Deng, Q. Zhang, H. C. Zhang, C. X. Zhang, W. H. Wang, Y. Gu, *Ind. Eng. Chem. Res.* **2014**, *53*, 1933; b) Q. Zhang, P. Yang, Y. Y. Deng, C. X. Zhang, R. Q. Zhu, Y. Gu, *RSC Adv.* **2015**, *5*, 103203.

[9] a) S. J. Cha, S. N. Cho, W. H. Lee, H. S. Chung, I. N. Kang, M. C. Suh, *Macromol. Rapid Commun.* **2014**, *35*, 807; b) H. K. Shih, Y. L. Chu, F. C. Chang, C. Y. Zhu, S. W. Kuo, *Polym. Chem.* **2015**, *6*, 6227.

[10] a) J. H. Fang, H. Kita, K. Okamoto, *Macromolecules* **2000**, *33*, 4639; b) T. Agag, C. R. Arza, F. H. J. Maurer, H. Ishida, *Macromolecules* **2010**, *43*, 2748.

[11] a) K. Hakala, J. M. J. Nuutinen, T. Straub, K. Rissanen, P. Vainiotalo, *Rapid Commun. Mass Spectrom.* **2002**, *16*, 1680; b) N. Nunez-Dallos, *Tetrahedron Lett.* **2012**, *53*, 530; c) L. Zhang, Y. J. Zhu, D. Li, M. Wang, H. B. Chen, J. S. Wu, *RSC Adv.* **2015**, *5*, 96879.

[12] a) J. H. Wu, W. C. Chen, G. S. Liou, *Polym. Chem.* **2016**, *7*, 1569; b) C. H. Lin, Y. S. Shih, M. W. Wang, C. Y. Tseng, T. Y. Juang, C. F. Wang, *RSC Adv.* **2014**, *4*, 8692.

[13] Z. Q. Yan, B. Xu, Y. J. Dong, W. J. Tian, A. W. Li, *Dyes Pigments* **2011**, *90*, 269.

[14] S. J. Chung, K. S. Kim, T. H. Lin, G. S. He, J. Swiatkiewicz, P. N. Prasad, *J. Phys. Chem. B* **1999**, *103*, 10741.

[15] P. Macak, Y. Luo, P. Norman, H. Agren, *J. Chem. Phys.* **2000**, *113*, 7055.

[16] G. K. Paul, J. Mwaura, A. A. Argun, P. Taranekar, J. R. Reynolds, *Macromolecules* **2006**, *39*, 7789.

[17] a) H. J. Xia, J. T. He, B. Xu, S. P. Wen, Y. W. Li, W. J. Tian, *Tetrahedron* **2008**, *64*, 5736; b) H. Lu, L. L. Feng, S. S. Li, J. Zhang, H. F. Lu, S. Y. Feng, *Macromolecules* **2015**, *48*, 476.

[18] H. Ishida, in *Handbook of Benzoxazine Resins* (Eds: H. Ishida, T. Agag), Elsevier, Amsterdam **2011**, Ch. 1, p. 3.

[19] a) L. C. Lin, H. J. Yen, Y. R. Kung, C. M. Leu, T. M. Lee, G. S. Liou, *J. Mater. Chem. C* **2014**, *2*, 7796; b) L. C. Lin, H. J. Yen, C. J. Chen, C. L. Tsai, G. S. Liou, *Chem. Commun.* **2014**, *50*, 13917.

